Author Manuscript

Author Manuscript

Author Manuscript

Author Manuscript

HHS Public Access

Author manuscript

Curr Biol. Author manuscript; available in PMC 2016 August 17.

Published in final edited form as:

Curr Biol. 2015 August 17; 25(16): 2099–2110. doi:10.1016/j.cub.2015.06.076.

Origin, Specification, and Plasticity of the Great Vessels of the Heart

Danielle Nagelberg[1], **Jinhu Wang**[2], **Rina Su**[1], **Jesús Torres-Vázquez**[1], **Kimara L. Targoff**[3], **Kenneth D. Poss**[2], and **Holger Knaut**[1,*]

[1]Skirball Institute of Biomolecular Medicine, New York University School of Medicine, 540 First Avenue, New York, NY 10016, USA

[2]Department of Cell Biology, Howard Hughes Medical Institute, Duke University Medical Center, 349 Nanaline Duke Building, Durham, NC 27710, USA

[3]College of Physicians and Surgeons, Columbia University Medical Center, 630 West 168th Street, New York, NY 10023, USA

SUMMARY

The pharyngeal arch arteries (PAAs) are a series of paired embryonic blood vessels that give rise to several major arteries that connect directly to the heart. During development, the PAAs emerge from *nkx2.5*-expressing mesodermal cells and connect the dorsal head vasculature to the outflow tract of the heart. Despite their central role in establishing the circulatory system, the embryonic origins of the PAA progenitors are only coarsely defined, and the factors that specify them and their regenerative potential are unclear. Using fate mapping and mutant analysis, we find that PAA progenitors are derived from the *tcf21* and *nkx2.5* double-positive head mesoderm and require these two transcription factors for their specification and survival. Unexpectedly, cell ablation shows that the *tcf21+*; *nkx2.5+* PAA progenitors are not required for PAA formation. We find that this compensation is due to the replacement of ablated *tcf21+*; *nkx2.5+* PAA cells by endothelial cells from the dorsal head vasculature. Together, these studies assign the embryonic origin of the great vessel progenitors to the interface between the pharyngeal and cardiac mesoderm, identify the transcription factor code required for their specification, and reveal an unexpected plasticity in the formation of the great vessels.

INTRODUCTION

During vascular development, endothelial cells invade the pharyngeal arches to form the arteries that will connect the heart to the dorsal aorta and establish the circulatory system of

*Correspondence: holger.knaut@med.nyu.edu.

AUTHOR CONTRIBUTIONS

D.N. and H.K. designed the study. D.N. performed the experiments. R.S. assisted with stainings. J.T.-V. provided reagents and input. J.W. and K.D.P. provided unpublished transgenic zebrafish lines and had key input on the manuscript. K.L.T. provided the unpublished *nkx2.5* mutant zebrafish line. D.N. and H.K. analyzed the data and wrote the manuscript. All authors participated in producing the final version of the manuscript.

SUPPLEMENTAL INFORMATION

Supplemental Information includes Supplemental Experimental Procedures, three figures, two tables, six movies, and one data file and can be found with this article online at http://dx.doi.org/10.1016/j.cub.2015.06.076.

Author Manuscript Author Manuscript Author Manuscript Author Manuscript

the embryo [1]. In mammals, the posterior pharyngeal arch arteries 3–6 (pPAAs) are subsequently remodeled to form the great vessels—the carotid arteries, the aortic arch, and the pulmonary arteries [2, 3]—and improper formation of the great vessels results in cardiac birth defects in humans [4]. Fate mapping studies in fish and mice indicate that cells in the secondary heart field contribute to the head and heart muscles and the endothelium of the pharyngeal arch arteries. In mice, clonal analysis suggests that distinct progenitor pools give rise to distinct portions of head and heart muscles [5–7]. In mice and fish, *nkx2.5*-expressing mesoderm gives rise to heart muscle as well as pPAA endothelium [8]. Together, these observations suggest that the head muscles, the heart, and the pharyngeal arch arteries share a common origin. This idea is also supported by overlapping gene expression patterns and genetic requirements in these head structures; several transcription factors and signaling molecules are co-expressed in head muscles, the heart, and the pharyngeal arch arteries [9, 10], and some of these are required in the progenitors of all three tissues to promote correct head muscle, heart, and pharyngeal arch artery formation [11–13] [14]. Similarly, the co-occurrence of craniofacial and cardiac birth defects also supports the idea of a shared origin of head structures and the heart [4, 15, 16]. For example, key features of the DiGeorge Syndrome are cardiac abnormalities, abnormal facies, and a cleft palate [17]. Together, these studies suggest that the pharyngeal arch arteries are derived from a large mesodermal population that also gives rise to head and heart muscle (reviewed in [18]). However, despite these observations, the exact origin of the great vessels/pPAAs, the mechanism of their specification, and their regenerative potential remain unclear.

Here, we show that the pPAA progenitors arise from a small population of head mesodermal cells that co-express the cardiac marker *nkx2.5* and the head myoblast marker *tcf21*. Consistent with this expression profile, we find that the pPAA progenitors also require the transcription factors *nkx2.5* and *tcf21* for their specification. However, in the absence of the pPAA progenitors, the pPAAs still form. We find that this surprising vascular plasticity is possible due to neighboring endothelial cells that migrate in and replace the missing pPAAs.

RESULTS

tcf21+ Cells Contribute to Head Muscles, the Ventral Head Vasculature, and the Heart

To understand the role of the pharyngeal mesoderm in pPAA development, we sought a genetic marker to visualize and manipulate this tissue [19]. Consistent with observations in chicken and mice [20–22], we find that the transcription factor *tcf21* (Epicardin/Capsulin/Pod1) is expressed bilaterally at the 12-somite stage (15 hpf) in two domains within the head mesoderm—an anterior domain and a posterior domain (Figure 1A). Using *tcf21:mCherry-NTR* (referred to as *tcf21:mCherry* if not indicated otherwise), a transcriptional reporter for *tcf21+* cells [23], we find that at the 14-somite stage (16 hpf), the anterior *tcf21* expression domain is bounded anteriorly by the prechordal plate mesoderm marked by *pitx2* [24] and overlaps posteriorly with the cardiac mesoderm marked by a transcriptional reporter for *nkx2.5* (*nkx2.5: ZsYellow*) [8, 25] (Figures 1D, 1J, and 1K). The posterior domain of *tcf21* expression overlaps anteriorly with the *nkx2.5*-expressing domain (Figures 1D and 1E; Movie S3). During the next day, *tcf21* expression refines to the cores of the pharyngeal arches, where it is surrounded by neural crest cells, and splits into dorsal and ventral

Author Manuscript Author Manuscript Author Manuscript Author Manuscript

clusters, which then divide further into smaller clusters (Figures 1G–1I). Later, mCherry from the *tcf21:mCherry* transgene labels most of the head muscles (Figures 1L, 1M, and 4A–4D) as suggested previously [20–22, 26, 27]. However, mCherry also labels some of the dorsal and most of the ventral head vasculature, including part of the lateral dorsal aorta (LDA), the hypobranchial arteries (HAs), the pPAAs, and parts of the ventral aorta (VA) (Figures 1N, 1O, 4Q–4T, and 5A–5D). As this part of the head vasculature does not express *tcf21* once formed, it is likely labeled by mCherry protein that perdures in the descendants of *tcf21+* cells. Together, this indicates that *tcf21* marks two populations of the head mesoderm and suggests that these two cell populations give rise to part of the muscles and vasculature of the head. To test this idea, we followed the fate of *tcf21+* cells using Cre-mediated fate mapping. We generated embryos that express tamoxifen-inducible CreERT2 recombinase from the *tcf21* promoter (*tcf21:CreERT2*) [27] and carry the *bactin2:RSG* indicator line (*bactin2:loxP-DsRed-STOP-loxP-EGFP*), which switches from RFP to GFP expression after excision of the loxP-flanked RFP sequence [28]. We incubated these double transgenic embryos with 4-hydroxytamoxifen (4-HT) from 9 to 24 hpf and scored for the presence of GFP clones at 4.5 dpf (Figure 2A). Consistent with the labeling of the muscles and the vasculature of the head by mCherry protein perdurance from the *tcf21:mCherry* transgene (Figures 1L–1O), this protocol labeled cells with GFP in pharyngeal arch-derived head muscles, in the endothelial cells of pPAAs 3–6, the HA, and the VA, as well as tissues in the cardiac outflow tract and ventricle (Figures 2B–2E). This corroborates the idea that *tcf21+* cells give rise not only to part of the head muscles but also to the ventral head vasculature.

tcf21+ Cells Are Required for Head Muscle Formation but Not for PAA Formation

Our finding that most of the muscles and ventral vasculature of the head are derived from *tcf21+* progenitors suggests that *tcf21+* cells should be required for formation of these tissues. To determine whether this prediction holds true, we analyzed embryos expressing a codon-optimized version of the bacterial enzyme nitroreductase (NTRo) from the *tcf21* promoter (*tcf21:mCherry-NTR*) [23]. NTR converts the non-toxic prodrug metronidazole (Mtz) to a cytotoxic, DNA-crosslinking agent. The NTR-Mtz system has been used successfully to ablate specific cell types in zebrafish larvae [30, 31]. We bathed *tcf21:mCherry-NTR* embryos in Mtz from 9 hpf to 48 hpf (Figure 3A) and found in most embryos that *tcf21+* cells, labeled in red by the *tcf21:mCherry-NTR* transgene, died between 36 hpf to 38 hpf (Figure S1A). No dying cells were observed in DMSO-treated *tcf21:mCherry-NTR* embryos or Mtz-treated non-transgenic embryos. Using this approach, we ablated *tcf21+* cells in *tcf21:mCherry-NTR* embryos also carrying the muscle-specific *α-actin:GFP* transgene. In such embryos, all pharyngeal arch-derived head muscles were lost while the eye and neck musculature was not affected (Figures 3B–3I, 3D′, 3E′, 3H′, and 3I′), and the cartilage was deformed but correctly patterned (Figures S1B–S1E). This is consistent with previous fate mapping studies which place the origin of the eye muscles in the prechordal plate mesoderm [32–34] and the origin of the neck muscles mostly in the somitic mesoderm [5, 35]. In stark contrast to the complete ablation of the pharyngeal head muscles, the ventral head vasculature was only slightly impaired in Mtz-treated *tcf21:mCherry-NTR* embryos at 5 dpf. Mtz-treated *tcf21:mCherry-NTR* embryos carrying the endothelium-specific *flk:GFP* transgene form the LDA, the VA, and all pPAAs (Figures 3J–

Author Manuscript Author Manuscript Author Manuscript Author Manuscript

3Q, 3L′, 3M′, 3P′, and 3Q′). By contrast, the HA is mostly missing and always fails to connect to the LDA (Figures 3N–3Q, 3P′, and 3Q′; Table S1).

The failure to ablate the ventral head vasculature is not due to the failure to ablate the *tcf21+* cells because fluorescent protein expression driven by the two ventral head endothelial progenitor markers *tcf21* and *nkx2.5* is almost always absent in Mtz-treated *flk:GFP; tcf21:mCherry-NTR* and *nkx2.5:ZsYellow; tcf21: mCherry-NTR* embryos (Figures 3J–3Q, 3L′, 3M′, 3P′, and 3Q′ and Figures 3R–3Y, 3T′, 3U′, 3X′, 3Y′, respectively). Moreover, following *tcf21+* cells in individual *tcf21:mCherry-NTR* embryos that co-express the endothelial marker *flt1:YFP* indicates that *tcf21+* cells are completely ablated at 2 dpf but that the pPAAs show few or no defects by 5 dpf (Figures S1F–S1M). This indicates that most of the ventral head vasculature is able to form without its progenitors, most likely explained by an alternate source cell population that compensates for the lost ventral head vasculature progenitors.

Tcf21 Is Required for Head Muscle Formation and Together with Nkx2.5 for Head Vasculature Formation

To determine whether *tcf21* itself is required for the formation of the head muscles and the ventral head endothelium, we generated a *tcf21* deletion mutant (Figure S2A). In *tcf21* mutant embryos, all head muscles with the exception of the eye and neck-homologous muscles are either missing or severely reduced. Some fibers of the intermandibularis anterior, the interhyoideii, and the most posterior head muscles are frequently still present (Figures 4A–4H, 4C′, 4D′, 4G′, and 4H′), while heart morphology and function do not show a discernible defect (Figures S2B, S2E, and S2H) and the cartilage is only mildly affected (Figures S2C, S2D, S2F, and S2G). Time-lapse microscopy shows that *tcf21+* cells are born in *tcf21* mutant embryos and initiate their migration into the pharyngeal arches. However, these cells begin to die around 26 hpf, such that by 60 hpf, few *tcf21+* muscle progenitors remain (Movie S1). This indicates that Tcf21 is not required for the initial specification and migration of *tcf21+* cells into the pharyngeal arches but rather for the survival of head muscle progenitors. These observations are consistent with findings in mice and flies where Tcf21 promotes—in mice together with its paralog musculin/MyoR—the specification and survival of progenitors for a subset of jaw muscles and longitudinal gut muscles, respectively [22, 36].

In contrast to the clear requirement for *tcf21* in the head muscles, the ventral head vasculature is only mildly affected in *tcf21* mutant embryos. While the hypobranchial artery often fails to connect completely or is misshapen, all pharyngeal arch arteries form and become eventually lumenized (Figures 4Q–4X, 4S′, 4T′, 4W′, 4X′, and 5R; Table S2). Since *tcf21+* cells contribute to both head muscle and head endothelium but only the head muscles require Tcf21 activity, it is likely that Tcf21 acts together with another transcription factor to promote specification and/or survival of *tcf21+* endothelial cells. One candidate for such a transcription factor is Nkx2.5, as a subset of the *tcf21+* cells co-express *nkx2.5* before mesoderm migration into the pharyngeal arches (Figures 1D and 1E). Moreover, *nkx2.5*-expressing (*nkx2.5+*) cells also contribute to the pPAAs [8], and perduring fluorescent proteins expressed from the *tcf21* and *nkx2.5* promoters co-label the ventral head

Author Manuscript Author Manuscript Author Manuscript Author Manuscript

endothelium (Figures 1L, 1M, 5A–5D, and 5D′). To test this idea, we analyzed the formation of the ventral head endothelium in *tcf21* mutant, *nkx2.5* mutant, and *tcf21*;*nkx2.5* double mutant embryos transgenic for *flk:mCherry* to label endothelial cells and *nkx2.5:ZsYellow* to label pPAA progenitors. In contrast to *nkx2.5* morpholino knockdown experiments [8], which have recently been reported to be error prone [37], we find that the pPAAs are present at 60 hpf in *tcf21* mutant, *nkx2.5* mutant, and *tcf21*;*nkx2.5* double mutant embryos, although pPAAs occasionally failed to lumenize in *nkx2.5* mutant, *tcf21* mutant, and *tcf21*;*nkx2.5* double mutant embryos (Figure 5R). This result indicates, unexpectedly, that *tcf21* and *nkx2.5* are not required for pPAA formation. However, our observation that non-*tcf21+* cells can compensate for ablated *tcf21+* pPAA progenitors in forming the pPAAs (Figures 3J–3Q, 3L′, 3M′, 3P′, and 3Q′) suggests that *tcf21* and *nkx2.5* might be required for pPAA progenitor formation but dispensable for other cells to compensate in pPAA formation. To address this possibility, we asked whether pPAA progenitors are specified, survive, and contribute to the pPAAs in *tcf21*;*nkx2.5* double mutant embryos. To assess specification, we tested whether pPAA progenitors initiate the expression of the endothelial differentiation marker *tie1* in *tcf21:mCherry* transgenic embryos [38, 39]. Although we find that a subset of the *tcf21+* cells express *tie1* in the pharyngeal arches at 36 hpf in all four genotypes—wild-type, *tcf21* mutant, *nkx2.5* mutant, and *tcf21*;*nkx2.5* double mutants—its expression is mostly absent from pharyngeal arches 3 and 4 and weaker in the pharyngeal arches 5 and 6 in *tcf21*;*nkx2.5* double mutant embryos compared to wild-type and *tcf21* or *nkx2.5* single mutant embryos (Figure S3 and see file ImageJscripts3.ijm in Data S1). This suggests that the pPAA progenitors are not fully specified in the absence of Tcf21 and Nkx2.5 activity.

To test for survival of pPAA progenitors, we followed *tcf21; nkx2.5* co-expressing cells in *tcf21:mCherry-NTR* and *nkx2.5:ZsYellow* double transgenic embryos by time-lapse microscopy. Such embryos have three differently labeled fluorescent cell populations: *nkx2.5+*-only cells, *tcf21+*-only cells, and *nkx2.5+*; *tcf21+* cells. To follow these three cell populations separately, we segmented the movies based on the fluorescence intensities of the *tcf21:mCherry-NTR* and *nkx2.5:ZsYellow* transgenes and assigned each cell population a pseudo color using a custom-written ImageJ script (see file ImageJscripts1.ijm in Data S1). This analysis shows that *nkx2.5+*; *tcf21+* pPAA progenitor cells die between 40 and 42 hpf in *tcf21*;*nkx2.5* double mutant embryos, but not in wild-type, *tcf21* mutant, or *nkx2.5* mutant embryos (Movie S2), suggesting that the failure in proper specification compromises the survival of pPAA progenitors 4–6 hr later.

We assessed the contribution of pPAA progenitors to the pPAAs in wild-type, *tcf21* mutant, *nkx2.5* mutant, and *tcf21; nkx2.5* double mutant embryos in two transgenic backgrounds: in the first, we used *flk:mCherry* as a marker for the pPAAs and *nkx2.5:ZsYellow* as a marker for the pPAA progenitors. In the second, we used *flk:GFP* as a marker for the pPAAs and *tcf21:mCherry* as a marker for the pPAA progenitors. Similar to what we see in wild-type embryos, we find that in *nkx2.5* mutant embryos, almost all pPAAs express ZsYellow from the *nkx2.5* promoter or mCherry from the *tcf21* promoter and are derived from pPAA progenitors (Figures 5A–5H, 5D′, 5H′, and 5Q; Figure S2I; see file ImageJscripts2.ijm in Data S1). Also, the pPAAs in *tcf21* mutant embryos are mostly composed of *nkx2.5+* and

Author Manuscript Author Manuscript Author Manuscript Author Manuscript

tcf21+ pPAA progenitors, although some embryos occasionally display a pPAA that is only partly composed of pPAA progenitors (Figures 5I–5L, 5Q, and S2I). In contrast, the pPAAs in *tcf21*;*nkx2.5* double mutant embryos are mostly devoid of pPAA progenitor cells, displaying a small contribution of *nkx2.5*+ and *tcf21*+ cells, if any, to the pPAAs (Figures 5M–5P, 5Q, and S2I). Similarly, the *nkx2.5*+ and *tcf21*+ HA progenitors are absent in *tcf21; nkx2.5* double mutant embryos. However, in contrast to the pPAAs that form in the absence of pPAA progenitors, the HA recovers only partly and never connects to the LDA in the absence of its progenitors (Figures 5O and 5P; Table S2). This suggests that in contrast to the pharyngeal head muscle progenitors, which require only Tcf21 activity for their formation, the pPAA and HA progenitors require the combined activity of Tcf21 and Nkx2.5 for their specification and survival, a requirement that is masked in the pPAAs by compensation by other cells in the absence of the pPAA progenitors.

The Pharyngeal Arch Arteries Are Derived from the Interface between the Pharyngeal and Cardiac Mesoderm

To locate more precisely where pPAA progenitors are born, we used time-lapse microscopy to follow *nkx2.5*+/*tcf21*+ cells in the head mesoderm from the 15-somite stage (16.5 hpf) to 44 hpf (Movie S3). Consistent with our expression analysis (Figure 1), *nkx2.5*+ cells are flanked anteriorly and posteriorly by *tcf21*+ cells, and cells at the borders between the expression domains co-express both transcription factors at the 15-somite stage. Thus, the expression of *tcf21* and *nkx2.5* delineate three different cell populations in the head mesoderm: *tcf21*+ cells, *nkx2.5*+ cells, and *tcf21*+/*nkx2.5*+ cells.

We followed these three cell populations separately by segmenting the movies based on the fluorescence intensities of the *tcf21:mCherry-NTR* and *nkx2.5:ZsYellow* transgenes and pseudo-coloring each cell population as described above (see ImageJscripts1.ijm in Data S1). This analysis shows that a few *nkx2.5*+ cells move medially to contribute to the heart while others move laterally and ventrally to form the pericardial sac. In contrast, the cells in the two *tcf21*+ domains move anteriorly with the cells in the posterior *tcf21* expression domain moving faster, such that by 24 hpf, the posterior cells almost reach the anterior cells and bridge the initial gap that was created by the *nkx2.5*+-only cells. During this migration toward the anterior, the *tcf21*+ and *tcf21*+/*nkx2.5*+ cells coalesce into individual clusters that then form the inner cores of the pharyngeal arches. The cells in the anterior *tcf21* expression domain contribute to the core of the first and second pharyngeal arch, while the cells in the posterior *tcf21* expression domain contribute to the posterior five pharyngeal arches and then form dorsal head muscles and part of the LDA. The *tcf21*/*nkx2.5* co-expressing cells from the borders between the *nkx2.5* and *tcf21* expression domains also move anteriorly, similar to the *tcf21*+ cells. However, in contrast to the *tcf21*+ cells, which populate the dorsal part of the inner core of the pharyngeal arches, the *tcf21*+/*nkx2.5*+ cells move to the ventral part of the pharyngeal arches and ultimately form ventral head muscles and the HA, the pPAAs, and the VA. These observations indicate that the progenitors of the ventral head vasculature, including the pPAA progenitors, originate from the anterior and posterior borders of the *nkx2.5* expression domain, where it overlaps with the *tcf21* expression domain.

Author Manuscript Author Manuscript Author Manuscript Author Manuscript

Dorsal Head Endothelial Cells Compensate for the Loss of Pharyngeal Arch Artery Progenitors

Although pPAA progenitors are lost in embryos with ablated *tcf21+* cells and in *tcf21–/–*; *nkx2.5 –/–* double mutant embryos, the pPAAs still form. To determine the cellular origin for this vascular plasticity, we reasoned that a likely source of the compensating cells in embryos with lost pPAA progenitors is other, nearby endothelial cells. To test this idea, we followed endothelial cells marked by *flk:GFP* or *flt1:YFP* in Mtz-treated non-*tcf21:mCherry-NTR* and *tcf21:mCherry-NTR* embryos. In wild-type embryos, the *tcf21+*/*nkx2.5+* pPAA progenitors migrate dorsally to connect with the LDA (Figures 6A and 6B; Movies S3 and S4). By contrast, in embryos with ablated pPAA progenitors, endothelial cells from either the LDA or the primary head sinus migrate in the opposite direction ventrally to fill in the missing pPAAs (Figures 6C and 6D; Movie S4). Co-staining for the pharyngeal endoderm shows that the compensating endothelial cells populate the same position in the pharyngeal arches in *tcf21+* cell-ablated embryos as the pPAAs in control embryos (Movie S5). This suggests that the dorsal head vasculature is the source for the compensating cells. To confirm this observation, we generated embryos that express the photoconvertible Kaede protein in a mosaic fashion in all endothelial cells. For this, we injected *UAS-Kaede* DNA into *cdh5:Gal4FF* transgenic embryos [40]. *cdh5* is a pan-endothelial marker [41], and Kaede protein changes its fluorescence after exposure to UV light from green to red [42]. We imaged these embryos at 48 hpf before and after photoconversion of a region of cells in the dorsal head vasculature using a 405-nm laser. We then allowed the embryos to develop for 24 hr and imaged the embryos again at 72 hpf to determine the position of the photoconverted cells (Figure 6E). Consistent with our time-lapse analysis, we find that in embryos with ablated pPAA progenitors, photoconverted red endothelial cells from the LDA and primary head sinus move ventrally to form the pPAAs (Figures 6F–6I). By contrast, photoconverted red endothelial cells from the LDA and primary head sinus do not move ventrally to contribute to the pPAAs in embryos in which the pPAA progenitors were not ablated (Figures 6J–6M). As in embryos with ablated pPAA progenitors, endothelial cells from the LDA and primary head sinus also restore the pPAAs in *tcf21–/–*; *nkx2.5 –/–* double mutants, in which the pPAA progenitors fail to specify properly and die; time-lapse analysis of embryos carrying the endothelial marker *flk:mCherry* and the pPAA progenitor marker *nkx2.5:ZsYellow* shows that endothelial cells from the dorsal head vasculature sprout and migrate ventrally from the dorsal head vasculature to form the pPAAs (Figures 6O, 6Q, and 6S; Movie S6). In contrast, in wild-type control embryos, the pPAAs are formed by the *nkx2.5+* pPAA progenitors (Figures 6N, 6P, and 6R; Movie S6). In *tcf21* mutant embryos, endothelial cells from the dorsal head vasculature occasionally contributed to the pPAAs, consistent with the observation that the pPAA progenitors are occasionally reduced in number in this genetic scenario (Figures 5I, 5J, and 5Q). Together, these observations indicate that the dorsal head vasculature is the source for the plasticity of the pPAAs in scenarios where the pPAA progenitors are absent.

DISCUSSION

Our results suggest a model in which *tcf21+*, *tcf21+*/*nkx2.5+*, and *nkx2.5+* mesoderm give rise to head muscles, much of the ventral head vasculature, and the heart (Figure 7).

Author Manuscript Author Manuscript Author Manuscript Author Manuscript

According to this model, the pharyngeal head muscle progenitors are born in the two domains of the *tcf21+* mesoderm that abut the *nkx2.5+* heart mesoderm at its anterior and posterior borders. The anterior and posterior borders of the heart mesoderm, where cells express both *tcf21* and *nkx2.5*, give rise to the progenitors of much of the ventral head vasculature and the ventral pharyngeal head muscles, with cells at the anterior border giving rise to the HA and cells at the posterior border forming the pPAAs. During pharyngeal arch formation, the *nkx2.5+* cells stream medially and laterally to contribute to the heart and the tissues of the pericardium, respectively, while the *tcf21+/nkx2.5+* vascular and muscle progenitors at the anterior and posterior borders move closer to each other and populate the ventral cores of the pharyngeal arches—the dorsal cores are populated by *tcf21+* head muscle progenitors. These morphogenetic movements bring the progenitors of the HA and pPAAs, respectively, anterior and dorsal to the forming heart and provide a cellular explanation for the co-occurrence of many craniofacial and cardiac birth defects [4, 15, 16].

The related cellular origins of the head muscles, ventral head vasculature, and part of the heart are also reflected on a molecular level. Our and others' genetic analyses show that the *tcf21+* pharyngeal head muscle progenitors require Tcf21 activity for their specification [22, 26]. Similarly, we find that the *tcf21+/nkx2.5+* vascular HA and pPAA progenitors require the joint activity of Tcf21 and Nkx2.5 for their specification, and previous studies have shown that Nkx2.5 is required for ventricular identity in the heart [43–46]. Together, these observations suggest that the different combinations of these two transcription factors divide the head mesoderm into three domains that give rise to three spatially and molecularly related structures: (1) the pharyngeal head muscles, (2) the HA and the pPAAs, and (3) part of the heart (Figure 7). This not only adds a molecular explanation to the cellular explanation for the co-occurrence of many craniofacial and cardiac birth defects [4] but also points to the molecular machinery that may be necessary to make pPAA progenitor cells in vitro.

Intriguingly, we find that embryos with ablated ventral head vascular progenitors remake their posterior pPAAs from endothelial cells in the dorsal head vasculature. The compensating blood vessels in embryos with ablated pPAAs invade the pharyngeal arches up to a day later and from the opposite direction than the developing pPAAs in wild-type embryos, suggesting that the molecular mechanism underlying this plasticity is distinct from the guidance program in wild-type embryos. In principle, there are several possible scenarios for how compensating endothelial cells are recruited to re-form the lost pPAAs. Dying pPAA progenitors could secrete an endothelial attractant that then recruits nearby endothelial cells. However, given the 24-hr time span over which the pPAAs are re-formed, it is also likely that the dying pPAA progenitors activate adjacent cells to express an endothelial attractant to recruit compensating endothelial cells. Alternatively, the wild-type PAAs could physically block dorsal endothelial cells from moving in, such that when the wild-type PAAs are lost, dorsal endothelial cells are unbounded and able to migrate in to form the missing arteries.

More generally, this vascular plasticity allows the embryo to correct for minor defects in pPAA development to sustain proper circulation. Since congenital heart defects affect almost 1% of births per year in the United States [47, 48], the heart and its associated great

Author Manuscript Author Manuscript Author Manuscript Author Manuscript

vessels seem to be especially vulnerable to genetic and traumatic perturbation, suggesting that such a vascular buffering capacity might be essential. Moreover, if this plasticity proves to be a broader theme in development and maintenance of the vasculature, it might explain why many genes expressed in endothelial cells do not seem to be essential [37] and may warrant a closer phenotypic analysis.

EXPERIMENTAL PROCEDURES

Zebrafish Strains

Embryos were staged as previously described [29]. *tcf21*$^{\Delta 236}$ (this study) and *nkx2.5*^{vu179} [44] homozygous mutant embryos were generated by inbreeding heterozygous adults. Mutant, heterozygous, and wild-type embryos were distinguished through PCR amplification of the mutated locus based on size for *tcf21*$^{\Delta 236}$ and based on restriction digest with HinfI (New England Biolabs) for *nkx2.5*. All vertebrate animal work was performed at the facilities of the Skirball Institute at the NYU Langone Medical Center (NYULMC). NYULMC Animal Care & Use Program is fully accredited by the Association for Assessment and Accreditation of Laboratory Animal Care International (AAALAC). The Animal Care and User Program at NYULMC is in full compliance with PHS policy, and the Assurance of Compliance Number with the PHS is A3435-01. This study was approved by the NYULMC Animal Care & Use Program under protocol no. 110805-03. For a complete list of zebrafish strains and genotyping protocols, see Supplemental Experimental Procedures.

Mtz/NTRo-Mediated Cell Ablation

For *tcf21*+-cell ablation, *tcf21:mCherryNTRo* embryos were bathed in embryo water containing 10 mM Mtz (Sigma, M1547) as previously described [49] from 9 hpf to 48 hpf—or in the case of movies beginning before 48 hpf, 9 hpf to 36hpf—and transferred to embryo water without Mtz until the embryos were analyzed or until 5 dpf. Live embryos were mounted in agar, and z stacks were collected on a Leica SP5 II confocal microscope. ImageJ (NIH) was used to create maximum projections of the z stacks.

Cre-Mediated Fate Mapping

For 4-hydroxytamoxifen (4-HT, Sigma Aldrich) labeling, 9 hpf *tcf21:Cre-ER*; *βactin2:RSG* embryos were placed in embryo medium with 4-HT added to a final concentration of 5 μM, from a 1 mM stock solution made in 100% ethanol. After 15 hr, embryos were washed and placed in embryo medium without 4-HT until the embryos were 4.5 dpf. Live embryos were mounted in agar, z stacks were collected on a Leica SP5 II confocal microscope and genotyped for the *tcf21* mutation. GFP-labeled cells were manually scored by visual inspection using ImageJ (NIH). Embryos with putative GFP-labeled muscle fibers and endothelial cells were fixed and co-stained for MHC and Cdh5, respectively, to confirm the identity of the GFP-labeled cells.

Kaede Photoconversion-Mediated Fate Mapping

To follow endothelial cells using photoconversion of Kaede, we injected *cdh5:Gal4FF* transgenic control embryos and *cdh5:Gal4FF; tcf21:mCherryNTRo* double transgenic

Author Manuscript Author Manuscript Author Manuscript Author Manuscript

embryos [40] with 30 ng/ul *pDestTol2pA2-UAS-Kaede* plasmid DNA [50] and 25 ng/ul *tol2* mRNA. Tol2 enhances the integration of DNA constructs flanked with *tol2 cis*-acting sites into the genome [51]. Selected 48 hpf embryos with transient expression of green fluorescent Kaede protein in the head vasculature were mounted in agar and imaged on a Leica SP5 II confocal microscope. Using the 405-nm laser line, Kaede protein in endothelial cells of the LDA and PHS was photoconverted from green fluorescence to red fluorescence, and the embryo was imaged again. Embryos were removed from the agar, raised to 72 hpf, mounted in agar again, and imaged live to record the position of the photoconverted, Kaede-expressing endothelial cells.

Live Imaging and Time-Lapse Imaging and Analysis

For live imaging, embryos were mounted in 0.5% low-melt agarose/fish water (0.3g/L Instant Ocean Salt, Marineland Labs). z stacks were collected with a Leica 203 water dipping lens (NA 0.5) or a Leica 403 water dipping lens (NA 0.8) and a Leica SP5 II confocal microscope equipped with HyD detectors (Leica Microsystems) and a heated stage (Warner Instruments). The temperature of the water bath was monitored and maintained between 27.9° C and 28.4° C. z stacks evaluated by image segmentation were collected in the photon-counting mode. Embryos were genotyped by PCR as described in Supplemental Experimental Procedures.

Heartbeat Frequency Measurements

For determining the heartbeat frequency, we counted the heartbeat of individual embryos three times for 15 s each and averaged the heartbeat frequency for each embryo.

Supplementary Material

Refer to Web version on PubMed Central for supplementary material.

ACKNOWLEDGMENTS

We thank L. Christiaen for critical comments and F. Fuentes and B. Sun for excellent fish care. We thank J. Hutt and past and present members of the H.K. and J.T.-V. laboratories for helpful input and discussion. We thank S. Schulte-Merker for providing the *flt1:YFP* and *cdh5:Gal4FF* lines and G. Burns and C. Burns for providing the *nkx2.5:ZsYellow* line. The MF20 and zn-8 monoclonal antibodies developed by D.A. Fischman and B. Trevarrow, respectively, were obtained from the Developmental Studies Hybridoma Bank, created by the NICHD of the NIH and maintained at The University of Iowa, Department of Biology. This work was supported by a March of Dimes grant #5-FY10-476 (to H.K.), a grant from NIH (R01-HL081674 to K.D.P.), a postdoctoral fellowship from American Heart Association (to J.W.), and an NIH grant HD007520 (to D.N.). The Leica SP5 II microscope, maintained by the Microscopy Core of New York University Langone Medical Center, was supported in part by grant S10 RR024708 from the National Center for Research Resources, NIH.

REFERENCES

1. Hiruma T, Nakajima Y, Nakamura H. Development of pharyngeal arch arteries in early mouse embryo. J. Anat. 2002; 201:15–29. [PubMed: 12171473]
2. Buckingham M, Meilhac S, Zaffran S. Building the mammalian heart from two sources of myocardial cells. Nat. Rev. Genet. 2005; 6:826–835. [PubMed: 16304598]
3. Anderson RH, Webb S, Brown NA, Lamers W, Moorman A. Development of the heart: (3) formation of the ventricular outflow tracts, arterial valves, and intrapericardial arterial trunks. Heart. 2003; 89:1110–1118. [PubMed: 12923046]

Author Manuscript Author Manuscript Author Manuscript Author Manuscript

4. Gittenberger-de Groot AC, Bartelings MM, Deruiter MC, Poelmann RE. Basics of cardiac development for the understanding of congenital heart malformations. Pediatr. Res. 2005; 57:169–176. [PubMed: 15611355]
5. Lescroart F, Hamou W, Francou A, Théveniau-Ruissy M, Kelly RG, Buckingham M. Clonal analysis reveals a common origin between nonsomite-derived neck muscles and heart myocardium. Proc. Natl. Acad. Sci. USA. 2015; 112:1446–1451. [PubMed: 25605943]
6. Lescroart F, Kelly RG, Le Garrec J-F, Nicolas J-F, Meilhac SM, Buckingham M. Clonal analysis reveals common lineage relationships between head muscles and second heart field derivatives in the mouse embryo. Development. 2010; 137:3269–3279. [PubMed: 20823066]
7. Lescroart F, Chabab S, Lin X, Rulands S, Paulissen C, Rodolosse A, Auer H, Achouri Y, Dubois C, Bondue A, et al. Early lineage restriction in temporally distinct populations of Mesp1 progenitors during mammalian heart development. Nat. Cell Biol. 2014; 16:829–840. [PubMed: 25150979]
8. Paffett-Lugassy N, Singh R, Nevis KR, Guner-Ataman B, O'Loughlin E, Jahangiri L, Harvey RP, Burns CG, Burns CE. Heart field origin of great vessel precursors relies on nkx2.5-mediated vasculo-genesis. Nat. Cell Biol. 2013; 15:1362–1369. [PubMed: 24161929]
9. Sun Y, Liang X, Najafi N, Cass M, Lin L, Cai C-L, Chen J, Evans SM. Islet 1 is expressed in distinct cardiovascular lineages, including pacemaker and coronary vascular cells. Dev. Biol. 2007; 304:286–296. [PubMed: 17258700]
10. Verzi MP, McCulley DJ, De Val S, Dodou E, Black BL. The right ventricle, outflow tract, and ventricular septum comprise a restricted expression domain within the secondary/anterior heart field. Dev. Biol. 2005; 287:134–145. [PubMed: 16188249]
11. Zhang Z, Huynh T, Baldini A. Mesodermal expression of Tbx1 is necessary and sufficient for pharyngeal arch and cardiac outflow tract development. Development. 2006; 133:3587–3595. [PubMed: 16914493]
12. Harel I, Maezawa Y, Avraham R, Rinon A, Ma H-Y, Cross JW, Leviatan N, Hegesh J, Roy A, Jacob-Hirsch J, et al. Pharyngeal mesoderm regulatory network controls cardiac and head muscle morphogenesis. Proc. Natl. Acad. Sci. USA. 2012; 109:18839–18844. [PubMed: 23112163]
13. Watanabe Y, Miyagawa-Tomita S, Vincent SD, Kelly RG, Moon AM, Buckingham ME. Role of mesodermal FGF8 and FGF10 overlaps in the development of the arterial pole of the heart and pharyngeal arch arteries. Circ. Res. 2010; 106:495–503. [PubMed: 20035084]
14. Kong P, Racedo SE, Macchiarulo S, Hu Z, Carpenter C, Guo T, Wang T, Zheng D, Morrow BE. Tbx1 is required autonomously for cell survival and fate in the pharyngeal core mesoderm to form the muscles of mastication. Hum. Mol. Genet. 2014; 23:4215–4231. [PubMed: 24705356]
15. Tzahor, E. Head muscle development.. In: Brand-Saberi, B., editor. Results and Problems in Cell Differentiation Results and Problems in Cell Differentiation. Springer Berlin Heidelberg; Berlin: 2014. p. 123-142.
16. Parker SE, Mai CT, Canfield MA, Rickard R, Wang Y, Meyer RE, Anderson P, Mason CA, Collins JS, Kirby RS, Correa A, National Birth Defects Prevention Network. Updated national birth prevalence estimates for selected birth defects in the United States, 2004-2006. Birth Defects Res. A Clin. Mol. Teratol. 2010; 88:1008–1016. [PubMed: 20878909]
17. Wilson DI, Burn J, Scambler P, Goodship J. DiGeorge syndrome: part of CATCH 22. J. Med. Genet. 1993; 30:852–856. [PubMed: 8230162]
18. Diogo R, Kelly RG, Christiaen L, Levine M, Ziermann JM, Molnar JL, Noden DM, Tzahor E. A new heart for a new head in vertebrate cardiopharyngeal evolution. Nature. 2015; 520:466–473. [PubMed: 25903628]
19. Tzahor E, Evans SM. Pharyngeal mesoderm development during embryogenesis: implications for both heart and head myogenesis. Cardiovasc. Res. 2011; 91:196–202. [PubMed: 21498416]
20. von Scheven G, Bothe I, Ahmed MU, Alvares LE, Dietrich S. Protein and genomic organisation of vertebrate MyoR and Capsulin genes and their expression during avian development. Gene Expr. Patterns. 2006; 6:383–393. [PubMed: 16412697]
21. Lu J, Richardson JA, Olson EN. Capsulin: a novel bHLH transcription factor expressed in epicardial progenitors and mesenchyme of visceral organs. Mech. Dev. 1998; 73:23–32. [PubMed: 9545521]

Author Manuscript Author Manuscript Author Manuscript Author Manuscript

22. Lu J-R, Bassel-Duby R, Hawkins A, Chang P, Valdez R, Wu H, Gan L, Shelton JM, Richardson JA, Olson EN. Control of facial muscle development by MyoR and capsulin. Science. 2002; 298:2378–2381. [PubMed: 12493912]
23. Wang J, Cao J, Dickson AL, Poss KD. Epicardial regeneration is guided by cardiac outflow tract and Hedgehog signalling. Nature. 2015; 522:226–230. [PubMed: 25938716]
24. Essner JJ, Branford WW, Zhang J, Yost HJ. Mesendoderm and left-right brain, heart and gut development are differentially regulated by pitx2 isoforms. Development. 2000; 127:1081–1093. [PubMed: 10662647]
25. Chen JN, Fishman MC. Zebrafish tinman homolog demarcates the heart field and initiates myocardial differentiation. Development. 1996; 122:3809–3816. [PubMed: 9012502]
26. Lee G-H, Chang M-Y, Hsu C-H, Chen Y-H. Essential roles of basic helix-loop-helix transcription factors, Capsulin and Musculin, during craniofacial myogenesis of zebrafish. Cell. Mol. Life Sci. 2011; 68:4065–4078. [PubMed: 21347725]
27. Kikuchi K, Gupta V, Wang J, Holdway JE, Wills AA, Fang Y, Poss KD. tcf21+ epicardial cells adopt non-myocardial fates during zebrafish heart development and regeneration. Development. 2011; 138:2895–2902. [PubMed: 21653610]
28. Kikuchi K, Holdway JE, Werdich AA, Anderson RM, Fang Y, Egnaczyk GF, Evans T, Macrae CA, Stainier DYR, Poss KD. Primary contribution to zebrafish heart regeneration by gata4(+) cardiomyocytes. Nature. 2010; 464:601–605. [PubMed: 20336144]
29. Kimmel CB, Ballard WW, Kimmel SR, Ullmann B, Schilling TF. Stages of embryonic development of the zebrafish. Dev. Dyn. 1995; 203:253–310. [PubMed: 8589427]
30. Pisharath H, Rhee JM, Swanson MA, Leach SD, Parsons MJ. Targeted ablation of beta cells in the embryonic zebrafish pancreas using E. coli nitroreductase. Mech. Dev. 2007; 124:218–229. [PubMed: 17223324]
31. Singh SP, Holdway JE, Poss KD. Regeneration of amputated zebrafish fin rays from de novo osteoblasts. Dev. Cell. 2012; 22:879–886. [PubMed: 22516203]
32. Adelmann H. The development of the prechordal plate and mesoderm of Amblystoma punctatum. J. Morphol. 1932; 54:1–67.
33. Wachtler F, Jacob HJ, Jacob M, Christ B. The extrinsic ocular muscles in birds are derived from the prechordal plate. Naturwissenschaften. 1984; 71:379–380. [PubMed: 6482980]
34. Wachtler F, Jacob M. Origin and development of the cranial skeletal muscles. Bibl. Anat. 1986; 29:24–46. [PubMed: 3729921]
35. Schilling TF, Kimmel CB. Musculoskeletal patterning in the pharyngeal segments of the zebrafish embryo. Development. 1997; 124:2945–2960. [PubMed: 9247337]
36. Ismat A, Schaub C, Reim I, Kirchner K, Schultheis D, Frasch M. HLH54F is required for the specification and migration of longitudinal gut muscle founders from the caudal mesoderm of Drosophila. Development. 2010; 137:3107–3117. [PubMed: 20736287]
37. Kok FO, Shin M, Ni C-W, Gupta A, Grosse AS, van Impel A, Kirchmaier BC, Peterson-Maduro J, Kourkoulis G, Male I, et al. Reverse genetic screening reveals poor correlation between morpholino-induced and mutant phenotypes in zebrafish. Dev. Cell. 2015; 32:97–108. [PubMed: 25533206]
38. Lyons MS, Bell B, Stainier D, Peters KG. Isolation of the zebrafish homologues for the tie-1 and tie-2 endothelium-specific receptor tyrosine kinases. Dev. Dyn. 1998; 212:133–140. [PubMed: 9603430]
39. Pham VN, Roman BL, Weinstein BM. Isolation and expression analysis of three zebrafish angiopoietin genes. Dev. Dyn. 2001; 221:470–474. [PubMed: 11500985]
40. Bussmann J, Wolfe SA, Siekmann AF. Arterial-venous network formation during brain vascularization involves hemodynamic regulation of chemokine signaling. Development. 2011; 138:1717–1726. [PubMed: 21429983]
41. Larson JD, Wadman SA, Chen E, Kerley L, Clark KJ, Eide M, Lippert S, Nasevicius A, Ekker SC, Hackett PB, Essner JJ. Expression of VE-cadherin in zebrafish embryos: a new tool to evaluate vascular development. Dev. Dyn. 2004; 231:204–213. [PubMed: 15305301]

Author Manuscript Author Manuscript Author Manuscript Author Manuscript

42. Ando R, Hama H, Yamamoto-Hino M, Mizuno H, Miyawaki A. An optical marker based on the UV-induced green-to-red photo-conversion of a fluorescent protein. Proc. Natl. Acad. Sci. USA. 2002; 99:12651–12656. [PubMed: 12271129]
43. Lyons I, Parsons LM, Hartley L, Li R, Andrews JE, Robb L, Harvey RP. Myogenic and morphogenetic defects in the heart tubes of murine embryos lacking the homeo box gene Nkx2-5. Genes Dev. 1995; 9:1654–1666. [PubMed: 7628699]
44. Targoff KL, Colombo S, George V, Schell T, Kim SH, Solnica-Krezel L, Yelon D. Nkx genes are essential for maintenance of ventricular identity. Development. 2013; 140:4203–4213. [PubMed: 24026123]
45. Biben C, Weber R, Kesteven S, Stanley E, McDonald L, Elliott DA, Barnett L, Köentgen F, Robb L, Feneley M, Harvey RP. Cardiac septal and valvular dysmorphogenesis in mice heterozygous for mutations in the homeobox gene Nkx2-5. Circ. Res. 2000; 87:888–895. [PubMed: 11073884]
46. Tanaka M, Schinke M, Liao HS, Yamasaki N, Izumo S. Nkx2.5 and Nkx2.6, homologs of Drosophila tinman, are required for development of the pharynx. Mol. Cell. Biol. 2001; 21:4391–4398. [PubMed: 11390666]
47. Hoffman JIE, Kaplan S. The incidence of congenital heart disease. J. Am. Coll. Cardiol. 2002; 39:1890–1900. [PubMed: 12084585]
48. Reller MD, Strickland MJ, Riehle-Colarusso T, Mahle WT, Correa A. Prevalence of congenital heart defects in metropolitan Atlanta, 1998-2005. J. Pediatr. 2008; 153:807–813. [PubMed: 18657826]
49. Curado S, Stainier DYR, Anderson RM. Nitroreductase-mediated cell/tissue ablation in zebrafish: a spatially and temporally controlled ablation method with applications in developmental and regeneration studies. Nat. Protoc. 2008; 3:948–954. [PubMed: 18536643]
50. Kwan KM, Fujimoto E, Grabher C, Mangum BD, Hardy ME, Campbell DS, Parant JM, Yost HJ, Kanki JP, Chien C-B. The Tol2kit: a multisite gateway-based construction kit for Tol2 transposon transgenesis constructs. Dev. Dyn. 2007; 236:3088–3099. [PubMed: 17937395]
51. Kawakami K. Tol2: a versatile gene transfer vector in vertebrates. Genome Biol. 2007; 8(Suppl 1):S7. [PubMed: 18047699]

Author Manuscript Author Manuscript Author Manuscript Author Manuscript

Highlights

- Great vessel progenitors are born within the pharyngeal and cardiac mesoderm
- Tcf21 and Nkx2.5 are required for the survival of the great vessel progenitors
- Great vessel formation is highly plastic

Author Manuscript Author Manuscript Author Manuscript Author Manuscript

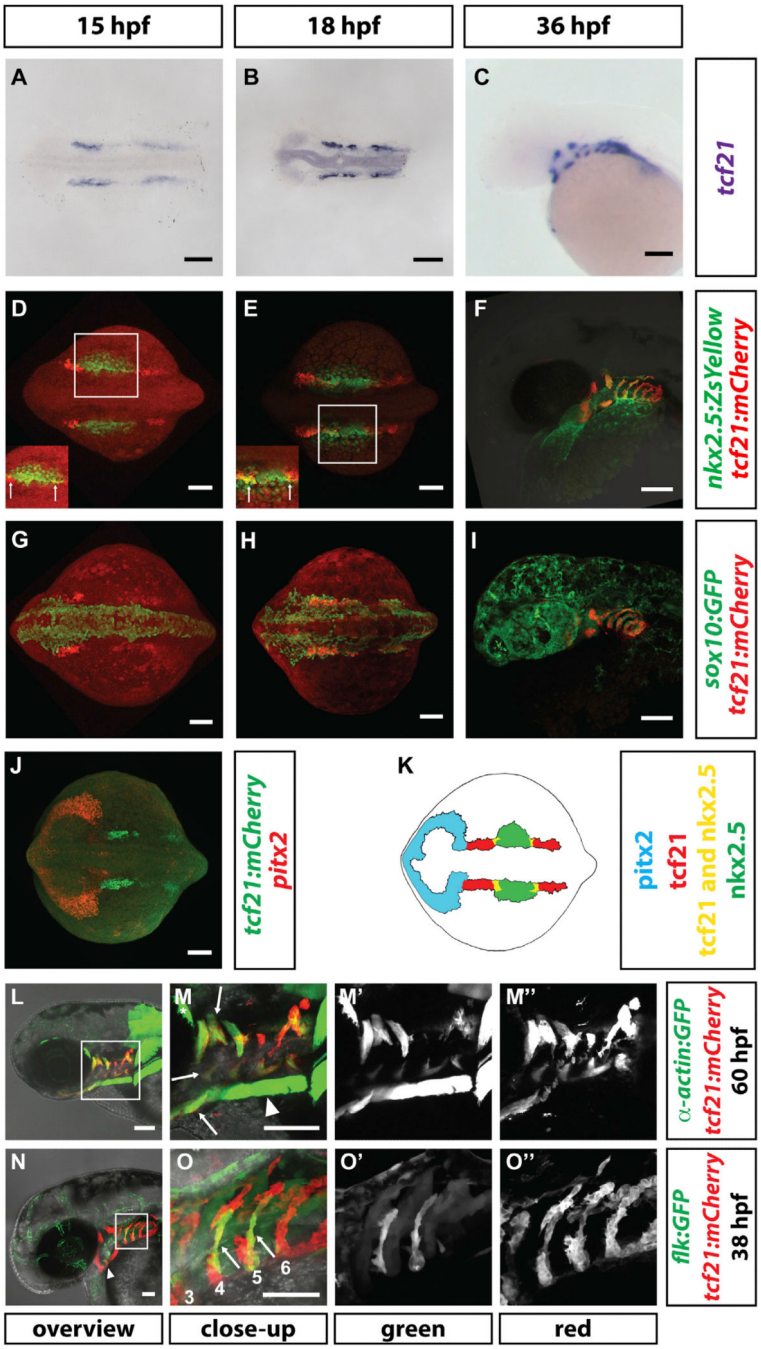

Figure 1. Expression of *tcf21* during Head Formation

(A–C) Staining of *tcf21* mRNA in wild-type embryos of indicated stages. n > 7.

(D–I) Images of fixed embryos of the indicated stages and genotypes stained for mCherry and ZsYellow proteins (D–F) or mCherry and GFP (G–I). White squares in (D) and (E) indicate region shown with increased intensity to demonstrate domain overlap in insets in (D) and (E). *sox10:GFP* was used to mark the neural crest contribution to the pharyngeal arches. Arrows in insets indicate region where *tcf21* and *nkx2.5* are co-expressed. n = 5 for (D) and (E); n = 1 for (F); n = 5 for (G); n = 2 for (H); n = 1 for (I).

Author Manuscript Author Manuscript Author Manuscript Author Manuscript

(J) Staining of *pitx2* mRNA and mCherry protein in a 15-somite stage embryo (n = 13).
(K) Schematic summary of *pitx2, tcf21*, and *nkx2.5* expression in the head mesoderm in the 14-somite stage embryo. Note that in this study, the term “head mesoderm” refers to the mesoderm comprised of the prechordal plate mesoderm, the pharyngeal mesoderm, and the cardiac mesoderm. *Pitx2, tcf21*, and *nkx2.5* mark—possibly only parts of—the prechordal plate, pharyngeal mesoderm, and pharyngeal mesoderm/secondary heart field mesoderm, respectively.
(L–M″) Live images of 60 hpf embryos carrying indicated transgenes. Square in (L) indicates magnified region in (M). (M′) and (M″) show single fluorescent channels. Arrows in (M) indicate some of the *tcf21+* muscles. Note that the prechordal plate-derived extraocular muscles (asterisk in M) and the somite-derived sternhyoideus muscles (arrowhead in M) do not express *tcf21*.
(N–O″) Live images of 38 hpf embryo carrying indicated transgenes. Square in (N) indicates magnified region in (O). (O′) and (O″) show single fluorescent channels. Arrowhead in (N) indicates the HA progenitors. Arrows in (O) indicate *tcf21+* pPAA progenitors, and the numbers label the arches. Note that the *flk:GFP* transgenic line weakly labels the pharyngeal endoderm and that PAA3 has already formed and lumenized and therefore is difficult to see in this projection.
Scale bars represent 100 μm (A–J, N, and O) or 50 μm (L and M). Anterior is to the left. Dorsal views (A, B, D, E, G, H, and J) and lateral views (C, F, I, and L–O).

Author Manuscript Author Manuscript Author Manuscript Author Manuscript

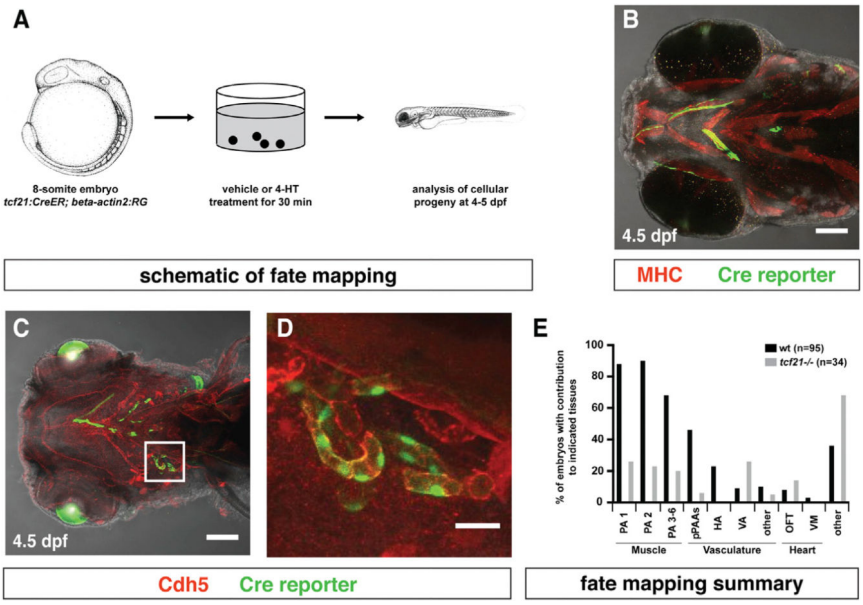

Figure 2. *tcf21*+ Cells Contribute to the Head Muscles, the Head Vasculature, and the Outflow Tract of the Heart

(A) Schematic representation of fate-mapping experiment. Images modified from [29].

(B) Image of *tcf21:CreER; bactin2:RSG* embryo stained for Myosin Heavy Chain and GFP to mark the head muscles and the Cre reporter, respectively.

(C and D) Image of *tcf21:CreER; bactin2:RSG* embryo stained for Cdh5 and GFP to mark the vasculature and the Cre reporter, respectively. Square in (C) indicates magnified region in (D) (n = 8).

(E) Summary of *tcf21*+ cell contributions to different tissues in wild-type embryos and in *tcf21* mutant embryos assessed by live confocal microscopy (wt embryos, n = 95; *tcf21* –/– embryos n = 34).

Scale bars represent 100 μm (B and C) and 10 μm (D). Anterior is to the left. Ventral views. From left to right: PA1, pharyngeal arch 1-derived skeletal muscle; PA2, pharyngeal arch 2-derived skeletal muscle; PA 3–6, skeletal muscle derived from PAs 3–6; pPAAs, pharyngeal arch arteries 3–6; HA, hypobranchial artery; VA, ventral aorta; other, other vascular labeling; OFT, outflow tract (myocardium, endothelium, smooth muscle, or epicardium); VM, ventricle (myocardium, endothelium, smooth muscle, or epicardium); other, cells derived from *tcf21*-expressing progenitors that we cannot unambiguously assign to a specific tissue.

Author Manuscript Author Manuscript Author Manuscript Author Manuscript

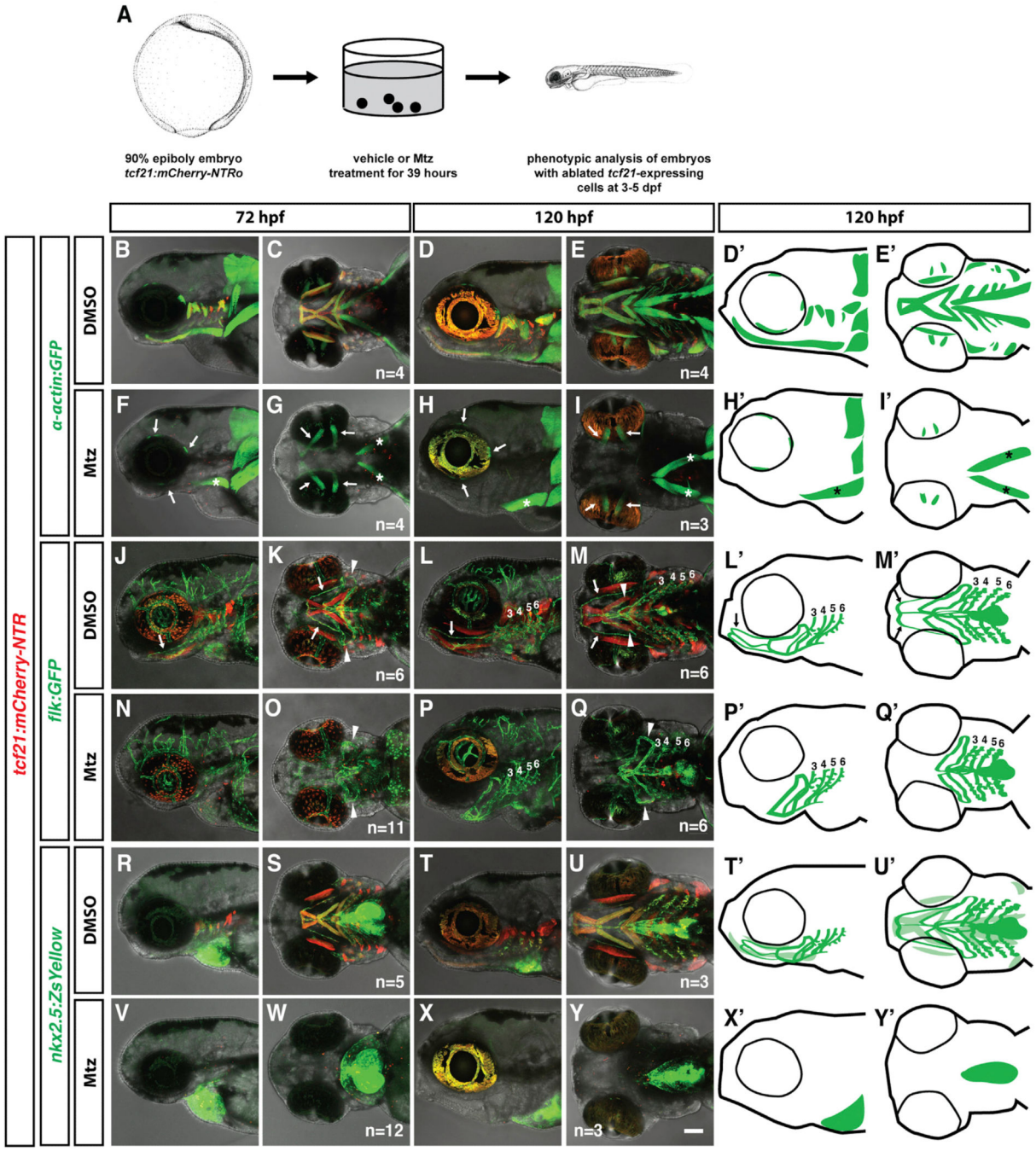

Figure 3. *tcf21+* cells Are Required for Head Muscle Formation but Not for Head Vasculature Formation

(A) Schematic representation of *tcf21+* cell ablation experiment. Images modified from [29]. (B–Y′) Live images and schematic diagrams of embryos of indicated stages carrying indicated transgenes treated with the vehicle control DMSO or Mtz as depicted in (A). Note that in (F)–(I), the prechordal plate-derived extraocular muscles (arrows in F–I) and the somite-derived sternohyoideus muscles (asterisks in F–I, H′, and I′) are not ablated. Arrows in (J)–(Q) indicate the HA; arrowheads point to the loop formed by the PAA 1 and the

Author Manuscript Author Manuscript Author Manuscript Author Manuscript

opercular artery, and numbers indicate PAAs 3–6. Note that the HA is missing in the *tcf21+* cell-ablated embryos. Note that in (V)–(Y) (schematic diagrams X′ and Y′), all *nkx2.5+* cells outside of the heart and pericardium are ablated. The light green color in (T′) and (U′) marks the *nkx2.5+* head muscles. The *nkx2.5+* endothelial cells are indicated by dark green. The scale bar represents 100 μm. Anterior is to the left. Lateral views (first, third, and fifth column) and ventral views (second, fourth, and sixth column). Sample number of imaged embryos is indicated as a total for the ventral and lateral views. See also Figure S1.

Author Manuscript Author Manuscript Author Manuscript Author Manuscript

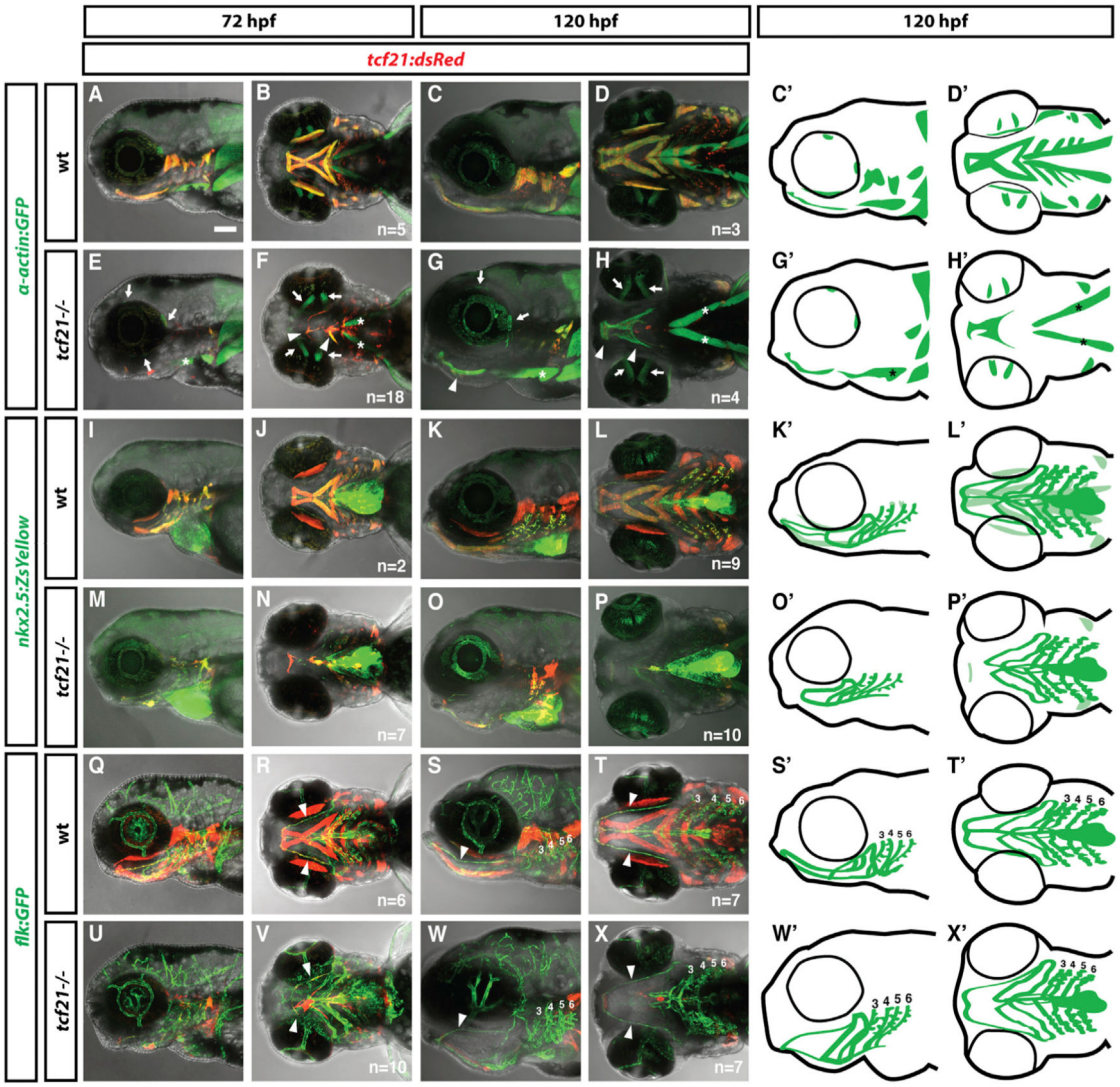

Figure 4. Specification of the Ventral Head Muscles Requires Tcf21 Activity

(A–X′) Live images and schematic diagrams of embryos of indicated stages and genotypes carrying the indicated transgenes. In mutants, most muscles expressing *tcf21* are absent or severely reduced (A–H, C′, D′, G′, H′). Extraocular muscles (arrows in E–H) and sternohyoideus muscles (asterisks in E–H, G′, H′) do not express *tcf21* and are not affected in *tcf21* mutant embryos. Arrowheads in (R)–(T) and (V)–(X) indicate the HA, and numbers indicate pPAAs 3–6. Note that the HA is formed incompletely in the *tcf21* mutant embryos (V, X, X′). The light green color in (K′) and (L′) marks the *nkx2.5*+ head muscles. The *nkx2.5*+ endothelial cells are indicated by dark green. Lateral views (first, third, and fifth column) and ventral views (second, fourth, and sixth column). Sample number of imaged embryos is indicated as a total for the ventral and lateral views.

Author Manuscript Author Manuscript Author Manuscript Author Manuscript

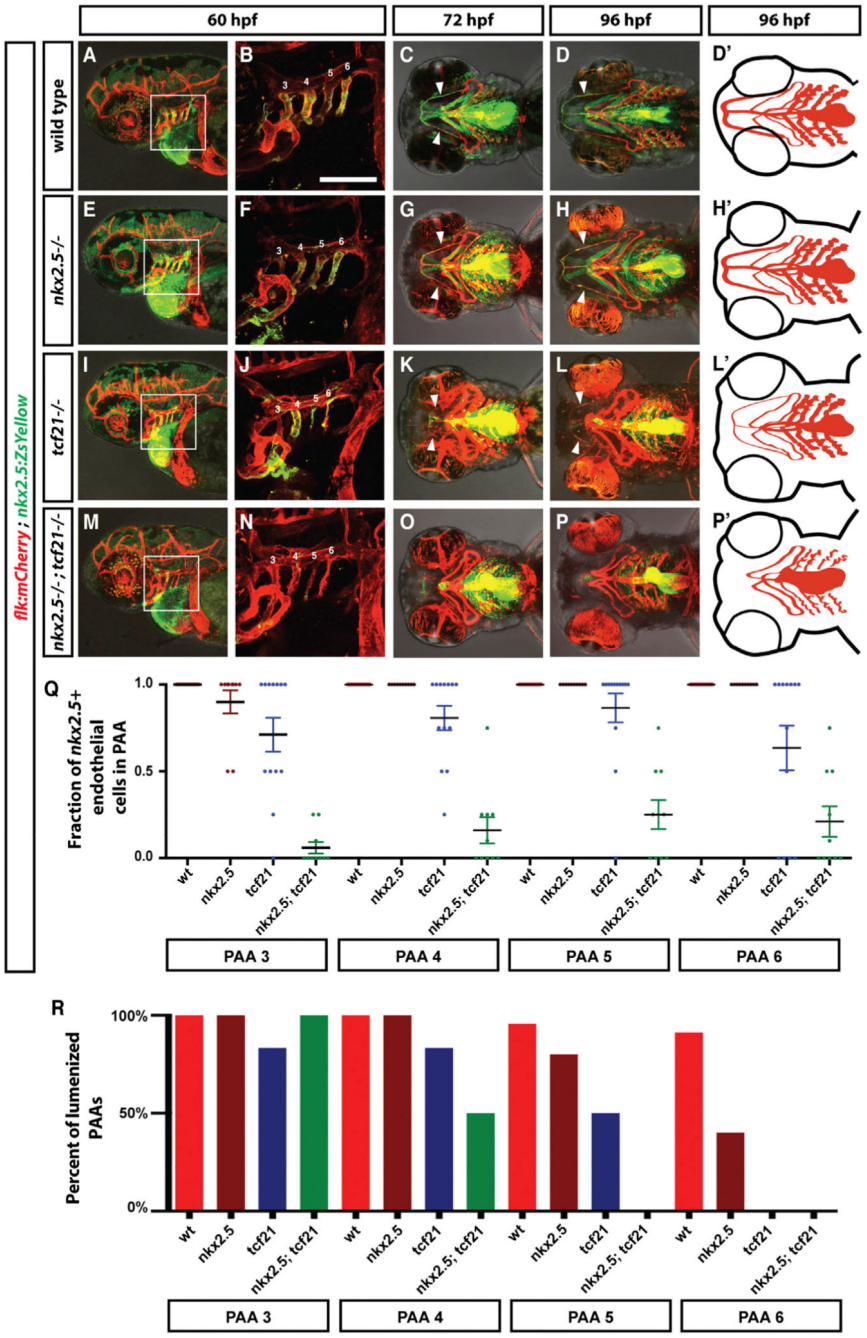

Figure 5. Specification of the Ventral Head Vasculature Requires the Combined Activities of Tcf21 and Nkx2.5

(A-P′) Live images and schematic diagrams of embryos of indicated stages and genotypes carrying the indicated transgenes. Squares in (A), (E), (I), and (M) indicate magnified regions shown in (B), (F), (J), and (N). Numbers indicate PAAs 3–6 in (B), (F), (J), and (N). Arrowheads indicates the HA. Lateral views (first and second column) and ventral views (third, fourth, and fifth column). Anterior is to the left. The scale bar represents 100 μm. Note that the images in (B), (F), (J), and (N) are thresholded using an ImageJ custom-written macro to only show the endothelial cells (see ImageJscripts2.ijm in Data S1).

Author Manuscript Author Manuscript Author Manuscript Author Manuscript

(Q) Quantification of the contribution of *nkx2.5*+ cells to the PAAs 3–6 in wild-type (includes *tcf21*−/+; *nkx2.5*−/+ and *tcf21*−/+; *nkx2.5*−/+ embryos, n = 37), *tcf21* mutant (includes *tcf21*–/–; *nkx2.5*−/+ embryos, n = 13), *nkx2.5* mutant (includes *nkx2.5*–/–; *tcf21*−/+ embryos, n = 10), and *tcf21; nkx2.5* double mutant embryos (n = 10). Individual data points and the mean with the SEM are indicated. See also Figures S2 and S3. In cases involving *tcf21; nkx2.5* double mutant embryos where contribution of *nkx2.5*+ cells to PAAs was ambiguous due to the presence of neighboring dying *nkx2.5*+ cells, scoring reflects a baseline assumption of *nkx2.5*+ cell contribution.

(R) Quantification of lumenized PAAs of indicated genotypes at 60 hpf. The sample numbers for each genotype are: wild-type embryos (includes *tcf21*−/+; *nkx2.5*−/+ and *tcf21*−/+; *nkx2.5*−/+ embryos) n = 19, *tcf21* mutants (includes *tcf21*–/–; *nkx2.5*−/+ embryos) n = 5, *nkx2.5* mutants (includes *nkx2.5*–/–; *tcf21*−/+ embryos) n = 7, and *tcf21*; *nkx2.5* double mutant embryos n = 3.

Author Manuscript Author Manuscript Author Manuscript Author Manuscript

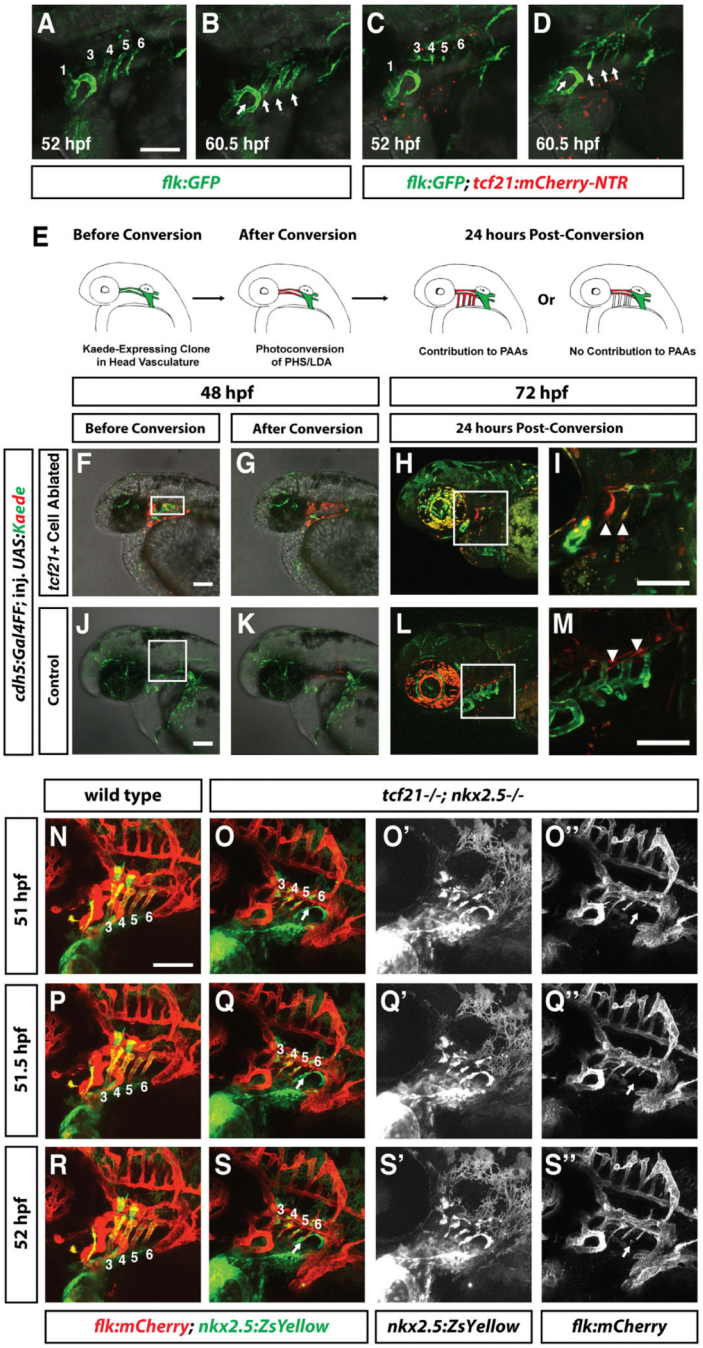

Figure 6. Endothelial Cells from the Dorsal Head Vasculature Compensate for Lost pPAAs in *tcf21* Cell-Ablated Embryos and *tcf21–/–; nkx2.5–/–* Embryos

(A–D) Live images of two embryos of indicated stages and genotypes carrying the indicated transgenes and treated with Mtz as described in Figure 3A. Numbers in (A) and (C) indicate the PAA, and arrows in (B) and (D) indicate the pPAAs. Images correspond to the first and last frames in Movie S4.

(E) Schematic of experimental design. *cdh5: Gal4FF; tcf21:mCherry-NTR* embryos were injected at the one-cell stage with *UAS-Kaede* DNA. The embryos were treated with Mtz to ablate the *tcf21+* cells as shown in Figure 3A. Embryos with green Kaede expression in the

Author Manuscript Author Manuscript Author Manuscript Author Manuscript

dorsal head vasculature were imaged, Kaede was photoconverted from green to red, and the contribution of endothelial cells in the dorsal head vasculature to the pPAAs was assessed 24 hr later.

(F) Mtz-treated *cdh5:Gal4FF; tcf21:mCherry-NTR* embryo with mosaic green Kaede expression in the head vasculature. Dying *tcf21+* cells are expressing mCherry protein.

(G) Same embryo as in (F), but Kaede-expressing endothelial cells in the dorsal head vasculature have been photoconverted from green to red. Region of photoconversion is marked by a rectangle in (F).

(H and I) Same embryo as in (F) 24 hr post-photoconversion. Photoconverted dorsal endothelial cells have migrated ventrally to compensate for the ablated pPAA progenitors and contribute to the pPAAs (arrowheads in I). Square in (H) indicates magnified region shown in (I) (n = 2).

(J) Mtz-treated *cdh5:Gal4FF* embryo not transgenic for *tcf21:mCherry-NTR* with mosaic green Kaede expression in the head vasculature (n = 8).

(K) Same embryo as in (J), but Kaede-expressing endothelial cells in the dorsal head vasculature have been photoconverted from green to red. Region of photoconversion is marked by a rectangle in (J).

(L and M) Same embryo as in (J) 24 hr post-photoconversion. Photoconverted, dorsal endothelial cells do not migrate ventrally and do not contribute to the pPAAs (arrowheads in M). Square in (L) indicates magnified region shown in (M).

Scale bars represent 100 μm. Anterior is to the left, and dorsal is up.

(N–S″) Live images of two embryos of indicated stages and genotypes carrying the indicated transgenes. Numbers in (N)–(S) indicate the PAA, and arrows in (O), (O″), (Q), (Q″), (S), and (S″) indicate endothelial cells that are migrating into arch 6 to form PAA 6. (O′), (Q′), and (S′) show the green channel only (*nkx2.5:ZsYellow*), and (O″), (Q″), and (S″) show the red channel only (*flk:mCherry*). Images correspond to time points 51, 51.5, and 52 hpf (frames 11, 12, and 13) in Movie S6. Lateral views. Anterior is to the left. Scale bars represent 100 μm.

Author Manuscript Author Manuscript Author Manuscript Author Manuscript

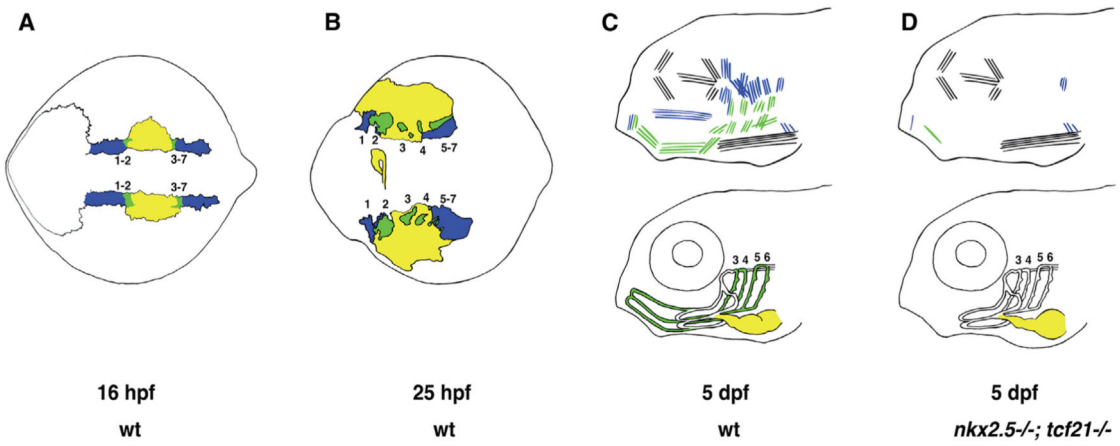

Figure 7. Schematic Depicting the Cellular Origin and Genetic Requirements for Head Muscle, Ventral Head Vasculature, and Heart Formation

(A) At 16 hpf (14 ss), *nkx2.5*+-only cells (yellow) are sandwiched between anterior and posterior domains of *tcf21*+ only cells (blue). *nkx2.5*+/*tcf21*+ cells (green) are found at the interface of the *nkx2.5*+ and *tcf21*+ domains, where these two domains overlap. Anterior *tcf21*+ and *nkx2.5*+/*tcf21*+ populations will give rise to the mesodermal cores of pharyngeal arches (PAs) 1 and 2, while posterior *tcf21*+ and *nkx2.5*+/*tcf21*+ populations will form the mesodermal cores of PAs 3–7. *nkx2.5*+/*tcf21*+ cells from the anterior domain will give rise mostly to the ventral head muscles derived from PAs 1–2 and the hypobranchial artery (HA), while *nkx2.5*+/*tcf21*+ cells from the posterior domain will give rise mostly to the ventral head muscles derived from PAs 3–7 and the posterior pharyngeal arch arteries 3–6 (pPAAs). *tcf21*+ cells from the anterior domain will give rise to dorsal and some ventral head muscles from PAs 1–2, while *tcf21*+ cells from the posterior domain will give rise to dorsal and some ventral head muscles from PAs 3–7. *nkx2.5*+ cells will give rise to the heart and pericardium. Dorsal view.

(B) As the PAs form, *tcf21*+ and *nkx2.5*+/*tcf21*+ cell clusters are found at the centers of each developing arch. *tcf21*+ cells predominate at the anterior and dorsal ends of PA1, the dorsal portions of PAs 2–6, and the dorsal and posterior portions of PA 7. *nkx2.5*+/*tcf21*+ cells predominate in the ventral portions of the developing arches. *nkx2.5*+ cells are found medially in the developing heart tube as well as laterally in the developing pericardium. Dorsal view.

(C) Top: *tcf21*+ cells give rise to dorsal muscles derived from PAs 1 to 7, as well as some ventral muscle fibers from PA 1 and PA 7. *nkx2.5*+/*tcf21*+ cells give rise to the ventral muscles as well as some dorsal muscle fibers of PAs 1–7. Eye and neck muscles are derived from non-*nkx2.5*/non-*tcf21* cells (black). Bottom: *nkx2.5*+ cells give rise to the heart. *nkx2.5*+/*tcf21*+ cells give rise to the HA, pPAAs 3–6, and the ventral aorta (VA). Pharyngeal arch artery 1 (PAA1), the opercular artery (ORA), and much of the LDA derive from non-*nkx2.5*-/non-*tcf21* cells (white). Part of the early LDA is derived from tcf21+ cells (data not shown). Lateral view.

(D) Top: *nkx2.5*–/–; *tcf21* –/– embryos lose most PA-derived muscles, with some fibers from PA 1- and PA 7-derived muscles remaining. Bottom: the HA is missing in *nkx2.5* –/–

embryos. pPAAs 3–6 are present but are now derived from compensating non-*nkx2.5*/non-*tcf21* cells originating in the dorsal head vasculature. Lateral view.

Author Manuscript Author Manuscript Author Manuscript Author Manuscript